PROGRESS ON INDUSTRIAL SOLAR CELL FRONT SIDE METALLIZATION BY PARALLEL DISPENSING TECHNOLOGY

M. Pospischil[a*], M .Kuchler[a], M. Klawitter[a], R. Efinger[a], C. Rodriguez[a], A. Padilla[a], H. Gentischer[a], M. König[b], M. Hörteis[b], L. Wende[c], A. Mette[d], F. Clement[a], R. Preu[a] and D. Biro[a]

a) Fraunhofer Institute for Solar Energy Systems ISE, Heidenhofstraße 2, 79110 Freiburg, Germany
b) Heraeus Deutschland GmbH & Co. KG, Heraeusstr. 12-14, 63450 Hanau, Germany
c) ASYS Automatisierungssysteme GmbH, Benzstr. 10, 89160 Dornstadt, Germany
d) Hanwha Q-Cells, GmbH, Sonnenallee 17 – 21, 06766 Bitterfeld-Wolfen OT Thalheim, Germany

ABSTRACT: This study summarizes the results of several medium scale cell experiments on the new dispensing machine, demonstrating cell efficiencies of up to 19.7% on industrial Cz Al-BSF material. Latest enhancement of the dispensing device further allowed for a significant reduction of wet paste laydown of down to 70 mg for the front contact finger grid which underlines the economic potential of the new technology. For the first time, state of the art contacting behavior could be demonstrated on parallel dispensed solar cells since the same screen printing paste was printed and dispensed. This fact, in combination with substantially improved finger homogeneity allows for increased Fill Factors at reduced paste consumption compared to screen printed reference solar cells.

Keywords: Silicon Solar Cell, Metallization, Dispensing

1 INTRODUCTION

Previous studies on dispensing as an alternative front side metallization process in crystalline silicon photovoltaics demonstrated how an adaption of paste rheology allows for a precise adjustment of contact finger geometry in a wide range [1, 2].

Furthermore, a substantially improved homogeneity of dispensed fingers compared to screen printed front side contacts results in more efficient material usage. Consequently, the use of dispensing technology leads to contact finger widths down to 27 µm at desired, high aspect ratios and without mesh marks and paste spreading, enabling high cell efficiencies like Lohmüller's demonstration of 20.6% in 2011 [3].

In order to demonstrate the benefit of these advantages, the analytical 2D simulative tool Gridmaster [4] was enhanced to observe the effect of various geometrical parameters on solar cell results and manufacturing costs [5]. Both however, imply a stable metallization process at high throughput rates. For this reason, a novel dispensing platform was developed, providing fully automated inline production feasibility. In the following, this platform was equipped with an advanced parallel dispensing print head as introduced in [2] and applied for extensive solar cell metallization on state of the art industrial Cz p-type material with high ohmic (R_{sh}~90Ω/sq.) emitters.

2 APPROACH

A significant advantage of dispensing compared with other metallization processes is its ability to directly apply pastes, that were developed for screen printing and thus ensure a reasonable contacting behaviour as well as proven long term stability of the grid pattern. Furthermore, the technology can be enhanced towards industrial applicability without the need to develop its own printing media in order to keep in pace with fast emerging screen printing paste development.

In this study, single and double screen printed contact grids with screen openings of just 45 µm and 40 µm, respectively were applied as references. The dispensing group was divided into one with a nozzle opening of 50µm using the exact same paste as the reference groups and two that use a rheologically adapted paste with 50 µm and 40 µm nozzle opening diameter, respectively (Fig. 1). The last four groups contain separately printed, non-contacting (floating) busbars [11] and thus follow a dual printing concept. All dispensed solar cells were produced using our ten nozzle parallel print head, which was mounted in a specially developed, inline applicable dispensing platform available from ASYS. After determination of the optimum fast firing temperature, the main experiment was performed at similar fast firing conditions. Finally, cell results were measured using an industrial inline cell tester followed by an investigation of the resulting contact geometries as well as C-DCR and TLM measurements.

Group	*S(1x)*	*S(2x)*	*D50S*	*D50R*	*D40R*
Material	Industrial pre-processed 156x156 mm² Cz p-type Si material, equipped with printed aluminum backsurfaces (Al-BSF)				
Busbars	Single screen print	Floating busbars, 3 x 1.2 mm			
Process		Double screen print	Dispensing with integrated ten nozzle parallel print head		
Opening (µm)	45	40	50	50	40
Paste	Screen printing paste (S)			Rheologically adapted (R)	
FFF	Fast firing at predetermined ideal temperature				
Charac.	IV-measurement, contact geometries, TLM				

Fig. 1: Single and double screen printed reference groups were compared with one dispensed group using the same paste, i.e. D50-S and two additional groups with a rheologically adapted paste at two different nozzle diameters, i.e. Disp.50-R and Disp.40-R, respectively.

3 RESULTS

3.1 Printed contact geometries

The resulting contact geometries were measured using a laser electron microscope (LEXT) that allows for an insitu determination of confocal and height information within a finger section of approximately 256 µm in length. An analysis of these geometrical data was

performed, using our in-house Matlab tool as mentioned in [9].
In Fig. 2, the most relevant geometrical data that are in direct correlation with cell results are plotted for the five groups, respectively. The electrical aspect ratio describes the ratio between average finger height and optical finger width and thus:

$$AR_{el} = \frac{h_{avg}}{w_o} = \frac{A_f}{w_o^2}$$

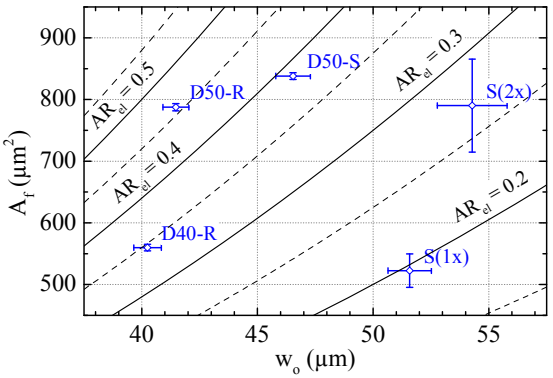

Fig. 2: Weighted average mean contact finger geometries on industrial Cz 156x156 mm² material regarding optical finger width w_o, electrical aspect ratio AR_{el}, and average finger cross section area A_f, The optical finger width here comprises the complete metal covered contact width of the finger.

All dispensed samples show a significantly reduced finger width, an increased aspect ratio, as well as an extremely low deviation in finger cross section area. This is another benefit of the contactless printing process that does not cause mesh marks on the cell. The finger cross section area of the dispensed samples with a nozzle opening of 50 µm is on a similar level to that of the double printed reference, the dispensed group with 40 µm nozzles is similar to the single screen printed reference. Since all samples were equipped with a constant number of contact fingers (N = 100), the finger cross section area is in direct correlation with wet paste consumption of the finger grid.

Comparing the two groups D50-S and D50-R, the rheologically adapted paste (-R) leads to a significant increase of aspect ratio and thus a further reduction of finger width using the same nozzle diameter. Due to a substantially higher shear rate inside the nozzle, the aspect ratio of the last group D40-R is lower than in D50-R. Consequently, the finger width of the corresponding solar cells is still larger than 35 µm, although record finger width of 27 µm were already demonstrated with the same nozzle configuration but a rheologically adapted paste of the previous generation [5].

3.2 IV results on Cz Al-BSF solar cells

Fill Factors above 80% indicate a good printing performance as well as contacting behavior of the applied pastes in all groups (Fig. 3). The slight decrease in FF of the last group results from a significantly reduced finger cross section area as well as finger widths that influence the total contact and grid resistance since the number of contact fingers N was not increased compared to the other two dispensing groups.

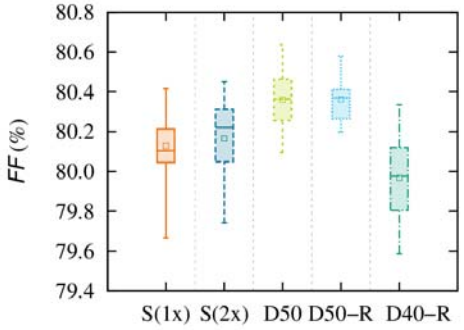

Fig. 3: Resulting Fill Factors FF for all five groups with the number of contact fingers $N_f = 100$ for all cells.

The V_{OC} of the groups following the dual printing concept is slightly increased compared to the single screen printed reference S(1x) due to reduced recombination losses underneath the non-contacting busbars (Fig. 4). The remaining differences between the groups result from different metal coverage that is proportional to the optical finger width w_o.

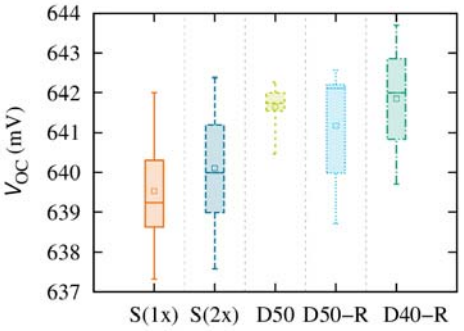

Fig. 4: Resulting open circuit voltage V_{oc} for all five groups.

This effect is even more visible when looking at the j_{SC}. Here, all three dispensing groups significantly exceed the two screen printed reference groups. Also the influence of paste rheology is clearly visible when comparing the values of D50 and D50-R.

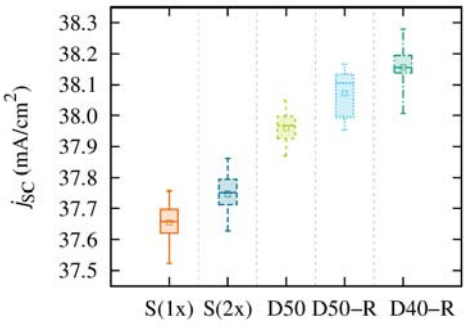

Fig. 5: Resulting short circuit current j_{sc} of the five groups. Relative increases correspond well with contact finger widths and additional effects from back reflection at the finger surface.

For the first time, dispensed solar cells exceed both reference groups in FF, V_{OC} and j_{SC}. Due to a constant number of contact fingers (N=100) solar cells dispensed with a nozzle diameter of only 40 µm revealed slightly lower FF values which however corresponds well with a drastically reduced wet paste laydown, see Fig. 6.

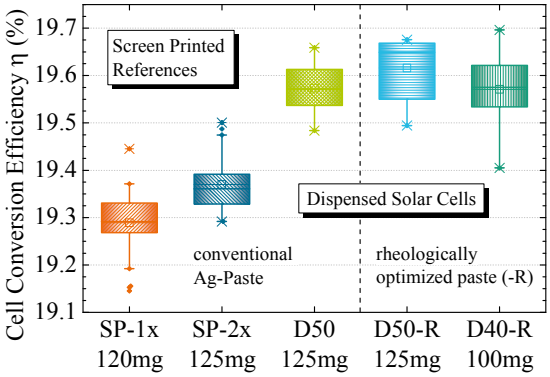

Fig. 6: Resulting cell efficiencies and total wet paste laydown of screen printed and dispensed solar cells.

Consequently, the resulting cell efficiencies show a significant increase of all dispensed samples compared to the screen printed references (Fig. 6). Here, top values of 19.7% on these Al-BSF samples demonstrate the potential of the technology as an alternative metallization concept. The median of the best dispensed group D50-R exceeds the single screen printed reference by approximately +0.4%abs. The total wet paste consumption of all groups is given in **Table I**.

Table I: Average wet paste laydown of busbars and contact fingers.

Group	*S(1x)*	*S(2x)*	*D50*	*D50-R*	*D40-R*
m_{BB} (mg)	~48	20	20	20	20
m_{Finger} (mg)	~72	105	105	105	80
Σm_{Grid} (mg)	120	125	125	125	100

In **Table II**, it is clearly visible that the differences in series resistance R_s between the groups can be directly attributed to differences in the finger grid resistance R_f. Thus, the two dispensed groups Disp.50 and Disp.50-R show the lowest values in R_s. Looking at the last group Disp.40-R, it is obvious that an additional contribution is caused by a significantly reduced metal contact area of these cells. The remaining contributions to R_s (i.e. $R_s - R_f$), that also include the contact resistance, remain similar for the all groups which proves the concept of directly applying pastes developed for screen printing in our dispensing device.

Table II: Distribution of area related series resistances R_s and finger resistance R_f.

Group	*S(1x)*	*S(2x)*	*D50*	*D50-R*	*D40-R*
R_s (Ωcm^2)	0.56	0.49	0.44	0.45	0.54
R_f (Ωcm^2)	0.22	0.15	0.11	0.12	0.18
$R_s - R_f$ (Ωcm^2)	0.34	0.34	0.33	0.33	0.36

3.3 TLM Results

The results from Rs analysis (**Table II**) imply homogeneous contacting behavior on industrial emitters of all five groups. In order to confirm this impression, randomly selected cells from each group were taken for a detailed contact resistance measurement by means of the transfer length method (TLM). Since the transfer length was higher than the contact width for all samples ($L_f > w_c$), a correlation between w_c and the specific contact resistance ρ_c could not be extracted. However, an interesting correlation was found between ρ_c and the contact height h_c, see Fig. 7.

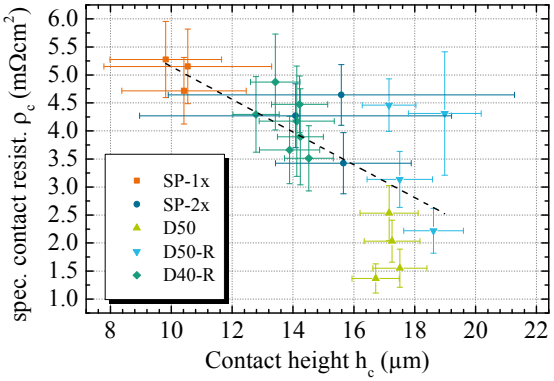

Fig. 7: Resulting specific contact resistance depending on contact height h_c. The linear trend line visualizes the influence the correlation between the two parameters.

Apparently, ρ_c decreases with increasing contact height h_c which was illustrated by a trend line in Fig. 7. This effect could be explained by the amount of glass frit available per unit area during the contact formation which increases with h_c. Consequently, the two groups D50 and D50-R provide the best contacting behavior, the single screen printed reference the worst with this paste. Finally, a slight difference between the group D50-R and D50 could be explained by an increased solid content in the former, rheologically adapted paste (-R) that slows down diffusion processes during the high temperature sinter step.

4 CONCLUSIONS AND OUTLOOK

Fast emerging thick film printing technologies remain a dynamic challenge for any kind of alternative metallization technology. The possibility to directly apply screen printing pastes however, allows for the enhancement of dispensing technology towards industrial cell processing. Consequently, increases in cell efficiencies of up to +0.4%abs. in comparison with standard single screen printing and +0.3%abs. with double printed reference were demonstrated on solar cells with industrial high-ohmic emitters. With the new developed, inline applicable dispensing platform, a continuous dispensing process was demonstrated at printing speeds up to 700 $mm \cdot s^{-1}$ and reasonable high yield values for a lab scale process. Towards an industrial application, the launching of a new developed 6'' dispense print head as well as the development of an intermittent operation of the device are the two major remaining challenges to be addressed.

5 ACKNOWLEDGMENTS

The authors would like to thank all co-workers at the Photovoltaic Technology Evaluation Center (PV-TEC) and the mechanical workshop at Fraunhofer ISE for processing of the samples. This work was partly supported by the German Federal Ministry for Economic Affairs and Energy within the research project "GECKO" under contract number 0325404.

6 REFERENCES

[1] M. Pospischil *et al.*, IEEE JPV **4**, 498 (2014).
[2] M. Pospischil *et al.*, Energy Procedia **43**, 111 (2013).
[3] E. Lohmüller *et al.*, IEEE Electron Device Letters **32**, 1719 (2011).
[4] T. Fellmeth, F. Clement, and D. Biro, Photovoltaics, IEEE Journal of **4**, 504 (2014).
[5] M. Pospischil *et al.*, Energy Procedia **55C**, 693 (2014).
[6] M. Pospischil *et al.*, in 39th IEEE PVSC (IEEE, Tampa, 2013).
[7] M. Pospischil *et al.*, in Photovoltaic Specialists Conference (PVSC), 2013 IEEE 39th2013), pp. 2250.
[8] J. Specht *et al.*, in Proceedings of the 25th European Photovoltaic Solar Energy Conference and ExhibitionValencia, Spain, 2010), pp. 1867.
[9] D.-H. Kim *et al.*, Materials Science and Engineering: B **177**, 217 (2012).
[10] M. Pospischil *et al.*, Energy Procedia **8**, 449 (2011).
[11] M. König *et al.*, Energy Procedia **27**, 1 (2012).